Electronic Supplementary Material (ESI) for Catalysis Science & Technology.
This journal is © The Royal Society of Chemistry 2022

Controllable assembly of Fe_3O_4-Fe_3C@MC by in-situ doping of Mn for CO_2 selective hydrogenation to light olefins

Pengze Zhang, Jingyu Yan, Fei Han, Xianliang Qiao, Qingxin Guan*, and Wei Li*

College of Chemistry, State Key Laboratory of Elemento-Organic Chemistry, Key Laboratory of Advanced Energy Materials Chemistry (Ministry of Education), Nankai University, No. 94 Weijin Road, Tianjin 300071, P. R. China.

1. Materials

$Fe(NO_3)_3 \cdot 9H_2O$ (98%), $Mn(NO_3)_2 \cdot 6H_2O$ (98%), and KNO_3 (99%) were purchased from Aladdin Ltd. (Shanghai, China). $Zr(NO_3)_4 \cdot 5H_2O$ was purchased from Xiya Chemical Technology Co., Ltd. $(NH_4)_{10}W_{12}O_{41} \sim xH_2O$ was purchased from Sigma–Aldrich (Shanghai) Trading Co., Ltd. Phenol (98%) and ethanol (99%) were purchased from Shanghai Merrill Chemical Technology Co., Ltd. (Shanghai, China). Formaldehyde (37%) was purchased from Xiya Chemical Technology (Shandong) Co., Ltd. (Linyi, China). Polyether F127 (molecular weight = 13000) was purchased from Tianjin Solomon Biotechnology Co., Ltd. (Tianjin, China). Boric acid (98%) was purchased from Tianjin Bohua Chemical Reagent Co., Ltd. (Tianjin, China). Phenolic resin (M≈500) was synthesized according to the literature [1].

2. Catalyst characterization

The structures of Fe-based catalysts were reported be changed during CO_2 hydrogenation reaction, so the catalysts of characterization were performed after the

catalytic performance evaluation.[2,3] The Fe content of the catalyst was analysed by X-ray fluorescence spectroscopy (Riguku supermini 200), with boric acid as a binder. The analysis of the specific surface area and pore size distribution of the catalyst was performed on a Microtrac BEL BELsorp-Max. Powder X-ray diffraction (XRD) of the catalyst was performed on a Riguku SmartLab 9 kW with a Cu Kα radiation source. The catalysts were reduced in a H_2 atmosphere at 350 °C before being characterized. The morphology of the catalyst was characterized by high-resolution field emission transmission electron microscopy (HR-TEM) and high-angle annular dark field-scanning transmission electron microscopy (HAADF–STEM) on an FEI Talos F200x with Super X.

H_2 temperature-programmed reduction (H_2-TPR), CO_2 temperature-programmed desorption (CO_2-TPD), and H_2 temperature-programmed desorption (H_2-TPD) were tested on a Micrometritics Autochem 2920. The H_2-TPR and CO_2-TPD tests were conducted after the sample was reduced at 350 °C with 50 mL/min 10% H_2/Ar mixed gas for 1.0 h and then purged with Ar (50 mL/min) for 1.0 h. The H_2-TPR test was conducted after the sample was heated at 350 °C with Ar (50 mL/min) for 1.0 h. The temperature program was increased from 50 to 800 °C at 10 °C/min. The chemical state of surface atoms was investigated by X-ray photoelectron spectroscopy (XPS) on a Thermo Scientific K-Alpha instrument equipped with an Al Kα source. The binding energy was calibrated using adventitious carbon (C 1 s peak at 284.8 eV). The catalysts were reduced in a H_2 atmosphere at 350 °C before being characterized.

3. Catalytic activity evaluation

The CO_2 hydrogenation reaction was performed in a fixed bed reactor (7.0 mm inner diameter), and the details of the reactor are given in Figure S1. Typically, 0.2 g catalyst (40–60 mesh) was used unless otherwise described. Before the activity evaluation, the catalyst was prereduced at H_2: 25 mL/min, 350 °C for 1.0 h. Subsequently, N_2 (50 mL/min) was used to purge the reactor, and the temperature of the reactor changed to meet the reaction requirements. Hereafter, the mixed gas of H_2, CO_2, and Ar (CO_2/H_2/Ar = 24:72:4) was fed into the reactor, and the pressure increased to 3.0 MPa gradually. All reacted gas mixtures were detected by online gas chromatography (Fuli GC9790II). CO_2, CO, CH_4, and Ar were analysed on a TCD detector with Haysep C and TDX–01 packed columns, and hydrocarbons and carbon hydroxides were analysed on an FID detector with an RB-1 capillary column. The date of GC is shown in Figure S13. The hydrocarbon distribution was calculated based on the total carbon moles (C-mole%). The carbon balance of the products was calculated to be above 95%. The catalytic performance was analysed after 8.0 hours of the reaction.

CO_2 conversion was calculated using equation (1):

$$CO_2\ Conversion\ (\%) = \frac{CO_{2\ in} - CO_{2\ out}}{CO_{2\ in}} \times 100\% \quad (1)$$

where the $CO_{2\ in}$ and $CO_{2\ out}$ represented the volume of flow in and out of the reactor.

CO selectivity was calculated by equation (2):

$$CO\ Selectivity\ (\%) = \frac{CO_{out}}{CO_{2\ in} - CO_{2\ out}} \times 100\% \quad (2)$$

where CO_{out} represents the CO volume of flow out of the reactor.

The selectivity of hydrocarbons in the whole hydrocarbon was calculated according

to equation (3):

$$C_i\ hydrocarbon\ selectivity\ (C-mol\%) = \frac{Mole\ of\ C_i\ hydrocarbon \times i}{\sum_{i=1}^{n} Mole\ of\ C_i\ hydrocarbon \times i} \times 100\% \quad (3)$$

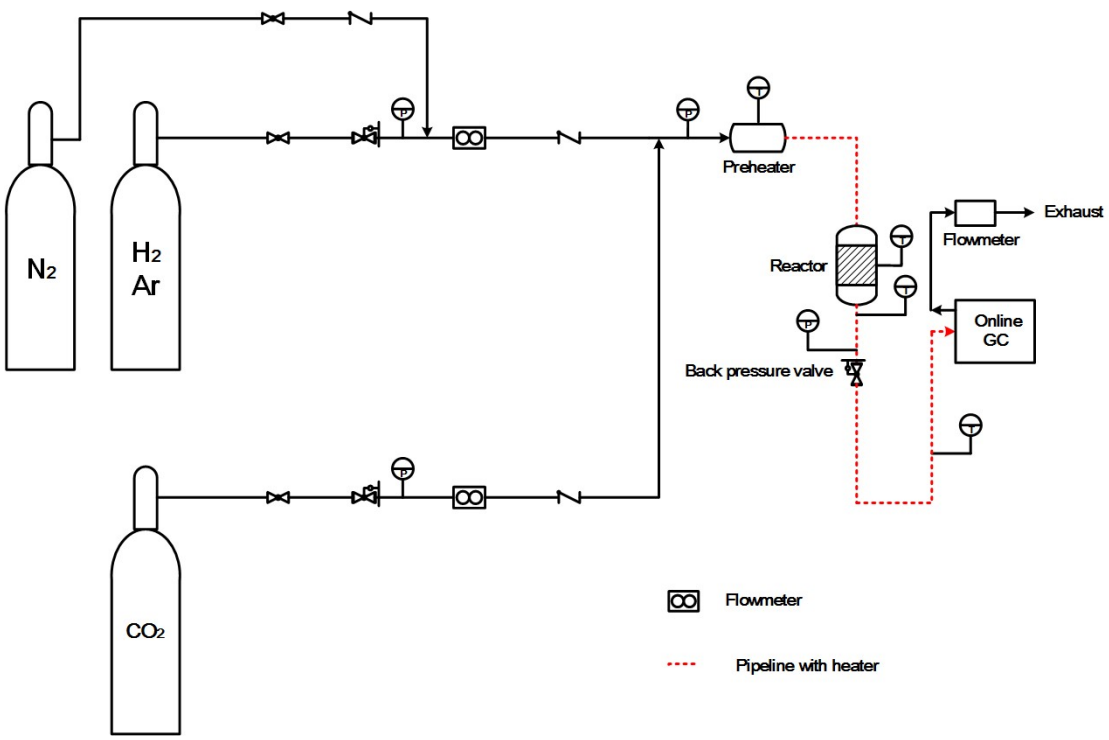

Figure S1. The schematic diagram of catalytic performance evaluation device.

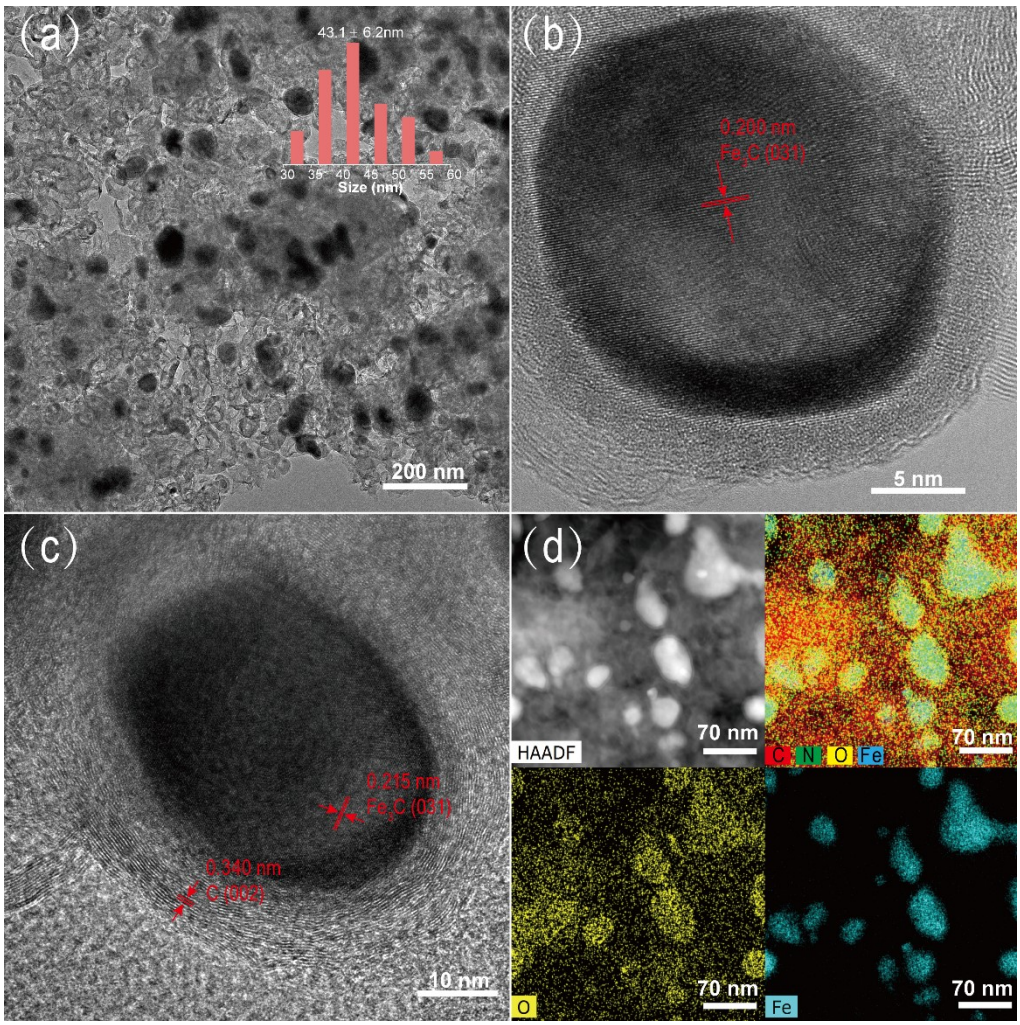

Figure S2. The HR-TEM images and HAADF-STEM images of 1.2Fe@MC.

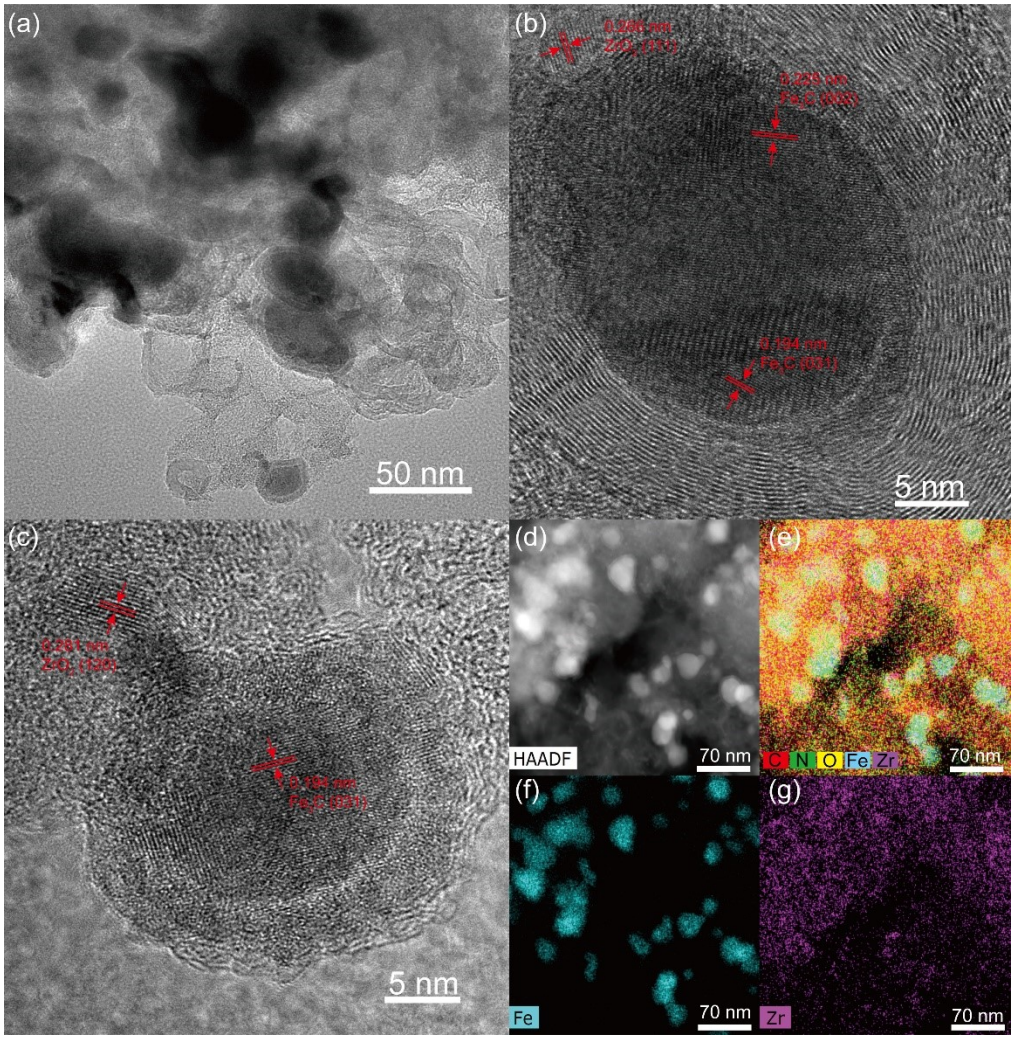

Figure S3. The HR-TEM images and HADDF-STEM images of 20%Zr-1.2Fe@MC.

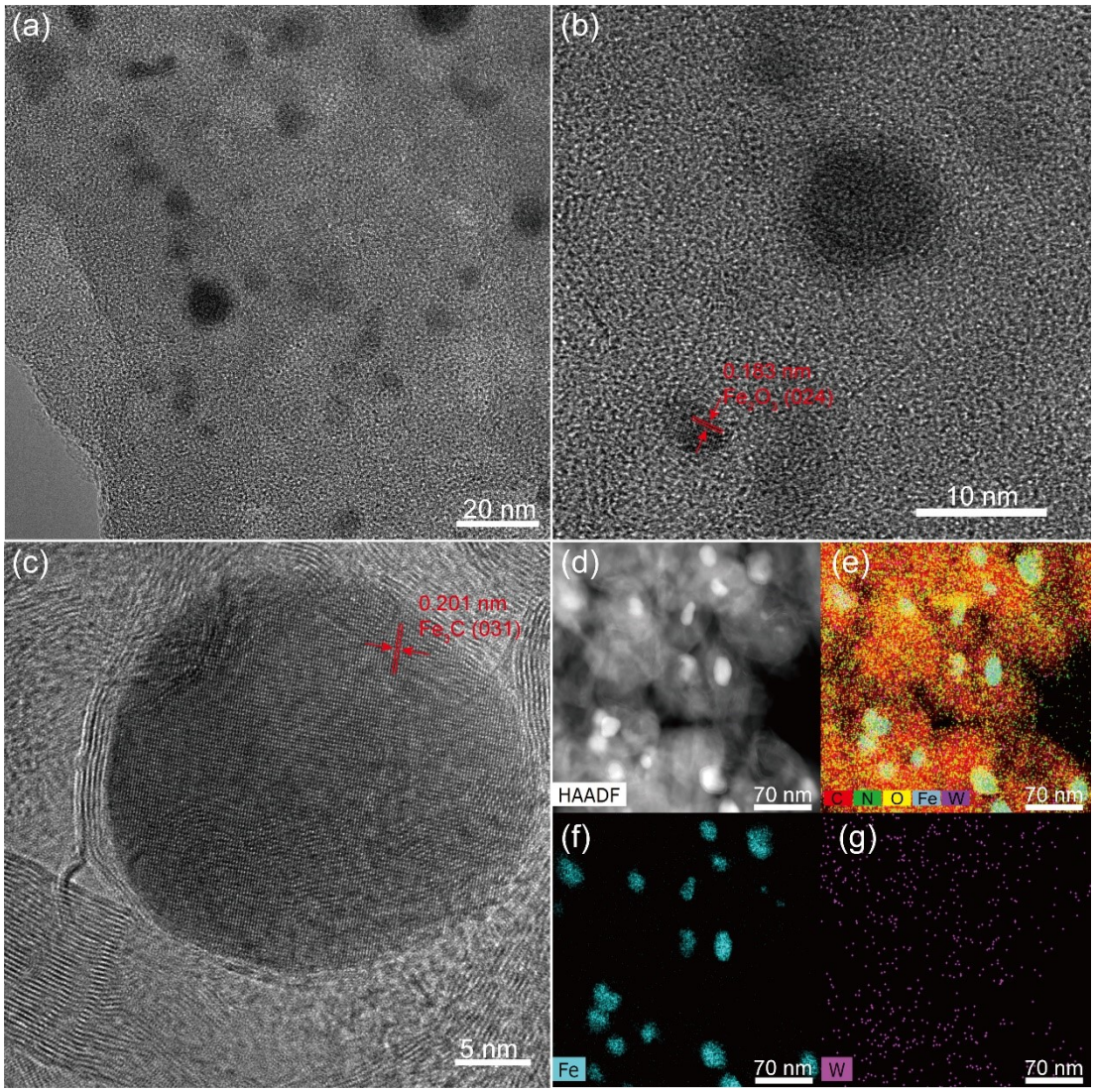

Figure S4. The HR-TEM images and HADDF-STEM images of 20%W-1.2Fe@MC.

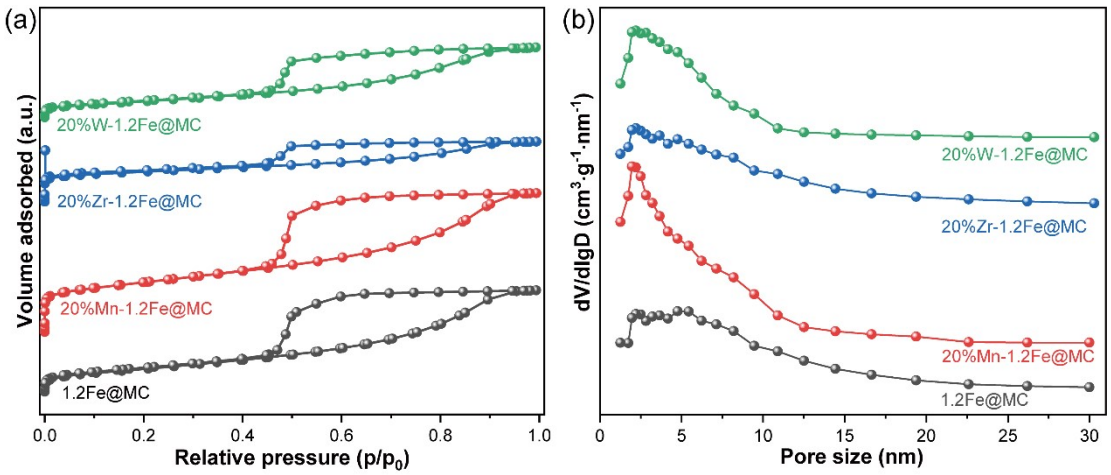

Figure S5. (a) The N_2-adsorption and desorption curve of 1.2Fe@MC, 20%Mn-1.2Fe@MC, 20%Zr-1.2Fe@MC, and 20%W-1.2Fe@MC. (b) The Pore size of

1.2Fe@MC, 20%Mn-1.2Fe@MC, 20%Zr-1.2Fe@MC, and 20%W-1.2Fe@MC.

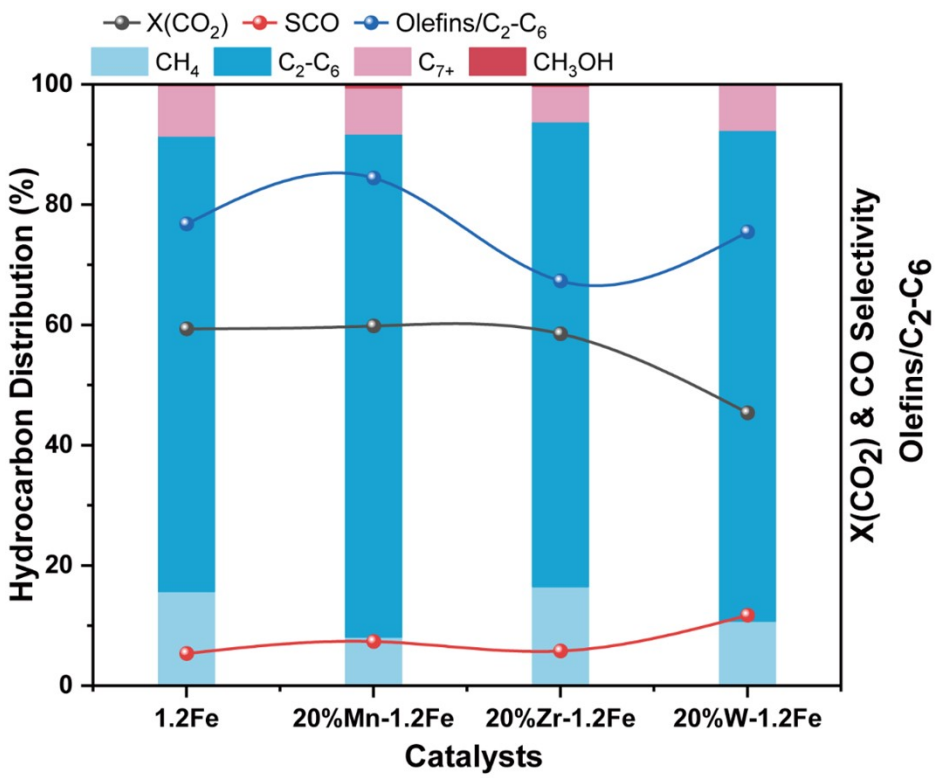

Figure S6. The catalytic performance of 1.2Fe@MC, 20%Mn-1.2Fe@MC, 20%Zr-1.2Fe@MC, and 20%W-1.2Fe@MC. Reaction conditions: 320 °C, 3.0MPa, GHSV = 12000 mL/g_{cat}/h.

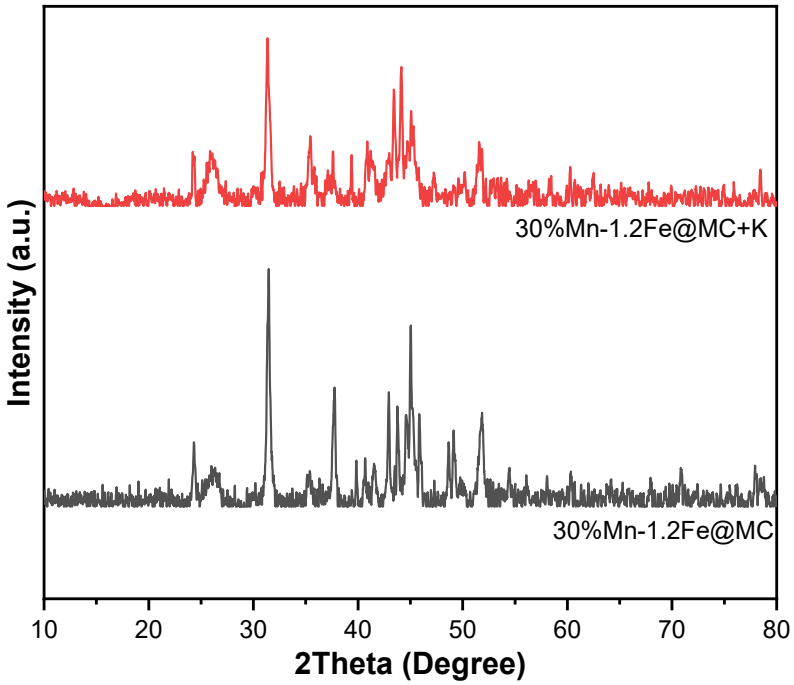

Figure S7. The XRD patterns of 30%Mn-1.2Fe@MC, 30%Mn-1.2Fe@MC+K.

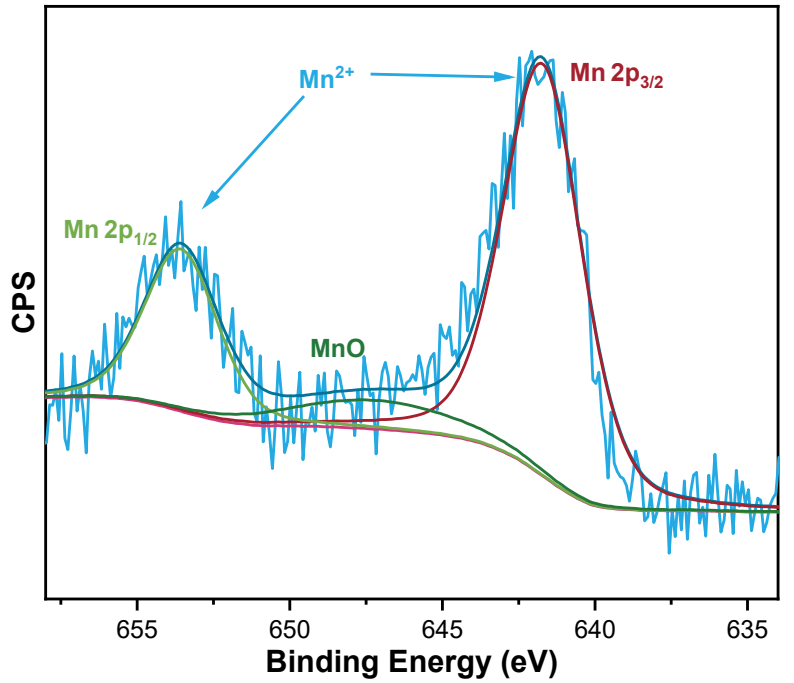

Figure S8. The Mn 2p XPS of 20%Mn-1.2Fe@MC

Table S1. The results of XPS peak fit

Fe 2p3/2 core			
Catalyst	BE (eV)	Concentration (atom%)	FeC_x/Fe_2O_3
1.2Fe@OMC	707.2	8.0	0.12
	708.3	2.7	
	711.0	73.1	
	713.0	16.1	
20%Mn-1.2Fe	707.2	10.5	0.18
	708.3	5.1	
	711.0	67.5	
	713.0	17.0	
20%Zr-1.2Fe	707.1	5.1	0.08
	708.1	2.5	
	710.8	74.2	
	713.0	18.2	
20%W-1.2Fe	707.3	4.7	0.07
	708.3	2.0	
	710.6	64.6	
	712.6	28.7	
30%Mn-1.2Fe	707.2	5.0	0.05
	708.3	0.0	
	711	68.1	

713	27.0	

Table S2. The textural properties of catalysts

Catalysts	$S_{BET}(m^2/g)$	Mean pore diameter(nm)	Pore volume(cm^3/g)
1.2Fe	204.5	5.3	0.37
20%Mn-1.2Fe	270.3	4.9	0.33
20%Zr-1.2Fe	299.4	3.39	0.35
20%W-1.2Fe	296.5	6.9	0.32
10%Mn-1.2Fe	305.6	4.53	0.35
30%Mn-1.2Fe	371.3	2.9	0.27

Table S3. The result of element Analysis

Catalyst	C	O	Fe	Mn	Zr	W
1.2Fe	92.23	7.24	15.44	-	-	-
20%Mn	88.81	10.4	13.53	4.41	-	-
30%Mn	-	-	12.66	5.88	-	-
20%Zr	90.33	9.7	11.72	-	6.02	-
20%W	91.28	8.27	10.10	-	-	8.74

Fe, Mn, Zr, and W (wt.%) element analysis was determined by X-ray fluorescence spectroscopy.

The C and O (atom. %) element analysis was decided by X-ray photoelectron spectroscopy.

Reference

[1] Y. Meng, D. Gu, F. Zhang, Y. Shi, H. Yang; Li Z., C. Yu, B. Tu; D. Zhao, *Angew. Chem. Int. Ed.,* 2005**, 44**, 7053.

[2] E. de Smit, F. Cinquini, A. M. Beale, O. V. Safonova, W. van Beek, P. Sautet and B. M. Weckhuysen, *J. Am. Chem. Soc.*, 2010, **132**, 14928.

[3] S. Li, J. Yang, C. Song, Q. Zhu, D. Xiao and D. Ma, *Adv. Mater.*, 2019, **31**, e1901796.